

Article

# Intelligent and Adaptive System for Welding Process Automation in T-Shaped Joints

Eider Aldalur <sup>1</sup>, Alfredo Suárez <sup>1</sup>, David Curiel <sup>2</sup>, Fernando Veiga <sup>1,2</sup> and Pedro Villanueva <sup>2,\*</sup>

<sup>1</sup> TECNALIA, Basque Research and Technology Alliance (BRTA), Science and Technology Park of Gipuzkoa, E20009 Donostia-San Sebastián, Spain; eider.aldalur@tecnalia.com (E.A.); alfredo.suarez@tecnalia.com (A.S.); fernando.veiga@unavarra.es (F.V.)

<sup>2</sup> Engineering Department, Public University of Navarra, Los Pinos Building, Arrosadía Campus, E31006 Pamplona, Navarra, Spain; david.curiel@unavarra.es

\* Correspondence: pedro.villanueva@unavarra.es

**Abstract:** The automation of welding processes requires the use of automated systems and equipment, in many cases industrial robotic systems, to carry out welding processes that previously required human intervention. Automation in the industry offers numerous advantages, such as increased efficiency and productivity, cost reduction, improved product quality, increased flexibility and safety, and greater adaptability of companies to market changes. The field of welding automation is currently undergoing a period of profound change due to a combination of technological, regulatory, and economic factors worldwide. Nowadays, the most relevant aspect of the welding industry is meeting customer requirements by satisfying their needs. To achieve this, the automation of the welding process through sensors and control algorithms ensures the quality of the parts and prevents errors, such as porosity, unfused areas, deformations, and excessive heat. This paper proposes an intelligent and adaptive system based on the measurement of welding joints using laser scanning and the subsequent analysis of the obtained point cloud to adapt welding trajectories. This study focuses on the optimization of T-joints under specific welding conditions and is intended as an initial implementation of the algorithm, thus establishing a basis to be worked on further for a broader welding application.

**Keywords:** welding; robotics; automation; thick joints



**Citation:** Aldalur, E.; Suárez, A.; Curiel, D.; Veiga, F.; Villanueva, P. Intelligent and Adaptive System for Welding Process Automation in T-Shaped Joints. *Metals* **2023**, *13*, 1532. <https://doi.org/10.3390/met13091532>

Academic Editor: Wei Zhou

Received: 28 July 2023

Revised: 26 August 2023

Accepted: 28 August 2023

Published: 29 August 2023



**Copyright:** © 2023 by the authors. Licensee MDPI, Basel, Switzerland. This article is an open access article distributed under the terms and conditions of the Creative Commons Attribution (CC BY) license (<https://creativecommons.org/licenses/by/4.0/>).

## 1. Introduction

A welded joint is defined as the union of two or more elements, creating continuity through heat and/or pressure with or without the use of filler material. Currently, there are numerous welding processes available, such as Gas Metal Arc Welding (GMAW) with a consumable electrode, which is the wire itself [1]; Flux Cored Arc Welding (FCAW) [2]; Gas Tungsten Arc Welding (GTAW) [3]; and Submerged Arc Welding (SAW) [4], among others. Among these processes, GMAW technology is widely used and will be employed in this work.

In certain industries, known as heavy industries (naval industry, oil and gas sector, energy sector, etc.), many components are large-scale mechanized and welded structures. For example, in the naval industry, the construction of large ships with lengths exceeding 24 m and internal volumes T.R.G. greater than 50 requires over 1000 h of welding. These joints can present some difficulties [5], including: (i) non-uniform and irregular pre-welded grooves, (ii) the need for certified and qualified welding operators, (iii) long deposition times, and (iv) welding positions that require special skills. Furthermore, in these types of sectors, there is often high physical demand and risk for the operator.

Specifically, within the different types of joints, welding thick joints has been shown in the literature to be one of the most challenging to automate, as they require multiple layers of deposited material to fill the joint [6]. Consequently, the current practice of manufacturing

thick-component joints has largely been limited to manual welding processes. Thus, the automation of welding using robotic systems has become an inevitable trend for this type of joint.

Until now, two main alternatives have been proposed for automating this type of welding, but complete automation has not been achieved. In the first alternative, the predefined welding paths are established using robotic welding configurations based on computer-aided design (CAD), where the welding solution can be planned, programmed, modified, and simulated offline with precise robotic kinematics and ideal (nominal) dimensions of the welds [7]. Systems that program manufacturing in advance clearly cannot predict or take into account the deformations and contractions that these types of parts undergo during layer-by-layer welding. Furthermore, deviations in geometry present in pre-welded joints cannot be considered solely by contemplating nominal dimensions that may not align with reality. Lastly, the exact positioning of the parts can also be inadequate due to incorrect assemblies or unforeseen displacement of the parts [8].

Second, there are methods based on scanning the joints and subsequently predicting the welding points, which generally consist of three stages. First, the geometric data of the joints are acquired through vision systems [9], and then they are processed to automatically select an optimal torch location. Next, precise tracking of the joints is performed, passing through the preselected optimal points [10]. Third, real-time defect detection is considered to assess whether the welds meet quality control requirements [11]. These processes are complex due to the high degree of automation required and algorithmic complexity. Other factors that also affect these processes are reflection problems with vision systems during welding caused by spectral signals [12], the sound of the arc [13], and the molten pool that can alter the scanned profile [14]. Another significant challenge in the automatic welding of thick plates is the contraction that the joint undergoes, leading to deformation as a result of high welding temperatures.

The solutions provided for robotic welding path generation span a range of approaches, including classical methods, such as arc detection, and novel techniques, such as multi-target programming. In addition, recent research has delved into intelligent path optimization strategies, which are poised to revolutionize the field. Through-arc sensing was developed for reciprocating wire feed gas metal arc welding, utilizing the welding voltage waveform to detect torch height and weld joint tracking, with voltage characteristics analyzed to reveal effective estimators for torch height sensing and reliable seam tracking achieved through voltage integration and a moving average algorithm [15]. Fridenfolk and Bolmsjö [16] addressed the challenges of joining ship sections in confined spaces. This classic approach utilizes control algorithms for seam tracking during welding, enhancing the adaptability of robotic systems to tolerate tolerances and variations in joint geometry. Kim [17] extended this concept by developing an arc sensor for reciprocating wire feed gas metal arc welding, leveraging voltage waveform characteristics to achieve torch height sensing and seam tracking.

Recent advancements in multi-objective programming have yielded substantial benefits. Zhou, Wang, and Gu [18] proposed a discrete MOEA/D with hybrid environment selection, optimizing welding paths based on path length and energy consumption. This technique showcases the power of optimization algorithms in achieving effective and efficient robotic welding processes. Ogbemhe, Mpofu, and Tlale [19] harnessed a hybrid multi-objective genetic algorithm to design trajectories that minimize discontinuities, ultimately enhancing tracking ability and process efficiency.

A survey by Wang, Zhou, Xia, and Gu [20] highlighted the strides in intelligent path optimization for welding robots. This study emphasizes the significance of automatic and efficient path optimization technologies to streamline robot path planning. This intelligent approach addresses the challenges posed by large-scale welding joints and welding seams, contributing to enhanced enterprise competitiveness, productivity, product quality, and reduced production costs.

Furthermore, Rout et al. [21] proposed an improved multi-objective ant lion optimizer for trajectory planning, considering kinematic and dynamic constraints. Their technique optimizes trajectories while balancing smoothness and productivity, exemplifying the potential of optimization algorithms in refining robotic motion planning.

Among these methods, “click and go” solutions can be found where the operator decides the most suitable welding point based on the information acquired by the vision system. This type of solution requires more operator intervention and can lead to errors, as the operator is presented with a limited set of profiles that may be insufficient to account for deformation along the entire joint. Additionally, manual point selection prolongs production time, making automatic selection through algorithms an improvement for the process, as it eliminates the need for an operator to select welding points for each layer.

This paper presents a system that takes the novelty of using profile scan data from a laser profilometric sensor to generate trajectories aligned with the robot’s coordinate system. In addition to improving accuracy, this approach has the dual capability of autonomous operation and collaborative human supervision. The fusion of unsupervised and operator-assisted functionality presents a compelling opportunity to drive the efficiency and adaptability of robotic welding processes to new heights. In this work, following the mentioned approach, to provide a fully automated, intelligent, and adaptive solution for welding thick joints, an automatic robotic system equipped with a laser profilometer and an algorithm for finding optimal welding positions was proposed. This system also checks the robot’s accessibility and movement consistency. More specifically, the main objective of this work was to define the torch’s trajectory automatically for welding the first layer of a thick joint based on the profiles of the joints acquired by the laser profilometer. This study initially targets the optimization of T-shaped joints within specific welding conditions. As we delve into this innovative realm, it becomes evident that certain pivotal facets require further exploration. One such facet pertains to the development of a comprehensive, perhaps dimensionless, process description capable of extending the method’s applicability across diverse scenarios. Moreover, a detailed exposition elucidating the automatic extension of the algorithm to accommodate varying parameters, encompassing joint size, material composition, and orientation, emerges as a logical progression. Additionally, a vital stride toward the robustness of this approach necessitates a comprehensive series of validation tests encompassing joints of varying sizes, materials, and orientations. By addressing these fundamental components, this study not only solidifies its relevance in the context of T-shaped joints but also lays a robust foundation for its extension to a broader spectrum of welding applications.

## 2. Materials and Methods

### 2.1. Materials

To validate and illustrate the development carried out in this work, “T”-shaped joints made of thick mild steel plates for oil and gas sector applications were analyzed and welded. These types of joints had the geometry depicted in Figure 1b, featuring a double-beveled joint that was pre-welded at the corners to ensure minimal deformations. The thickness of the plates was 60 mm, and the bevel angle was 45 degrees. A commercially available ER70S-6 steel wire with a diameter of 1.2 mm was used for welding.

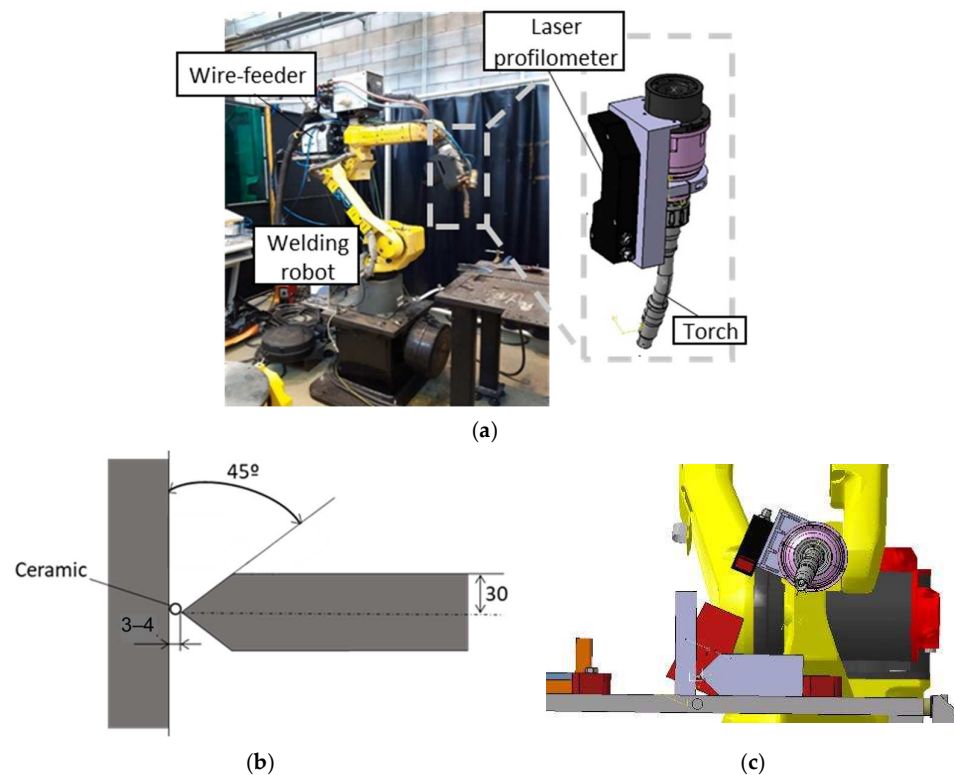


**Figure 1.** (a) Robotic welding set-up, (b) representation of the thick joint with T-shaped geometry, and (c) diagram of the joint scanning process using the laser profilometer.

## 2.2. Set-Up

In this work, to develop an intelligent and adaptive welding system based on joint scanning, a robotic cell designed to provide precise and reliable welds was used, as shown in Figure 1a. This cell consisted of a Titan XQ 400 AC Puls welding generator with a BUSINTX11 Profibus interface (EWM), which powers the GMAW welding torch mounted on the Fanuc Arc Mate 100-iC robotic arm. This setup was also equipped with the M drive 4 Rob5 XR RE wire feeder (EWM) and a shielding gas system [22].

For joint scanning, a Queltech Q4-120 laser profilometer was installed on the welding torch. It is a high-precision device designed to measure the three-dimensional shape of objects. It has a range of 120 mm on the Z-axis, 70 mm on the X-axis, a working distance of 84 mm, and a resolution of 0.0798 mm. The scanning position of the robot is shown in Figure 1c.

For welding, a 17 mm diameter nozzle and a Stick-out (the distance the wire extends from the nozzle) of 17 mm were used. As a shielding gas, a mixture of 80% argon and 20% carbon dioxide was introduced into the torch, with a flow rate of 17 L/min.

## 2.3. Data Acquisition Chain

To communicate the different elements that make up this intelligent and adaptive welding system, consisting of the robot, the monitoring application, the database, and the laser profilometer, a device-dependent communication configuration was established, as shown in Figure 2a. In this system, process monitoring was carried out using an open-loop control. For this purpose, the laser profilometer was installed as an external sensor, and the internal signals of the welding machine were also collected: current, voltage, wire feed speed, and travel speed. The positions of the robot axes and the wrist angles with respect to the coordinates of the workpiece were also monitored. Figure 2b illustrates the 3D joint geometry in the torch coordinate system, providing a representation of the joint geometry as perceived from the torch's perspective. On the other hand, Figure 2c depicts the profile captured by the sensor in its own coordinate system. This depiction offers insight into

the joint profile from the sensor's point of view. Therefore, while Figure 2b portrays the geometry's appearance from the torch, Figure 2c reveals the profile perception as captured by the sensor.

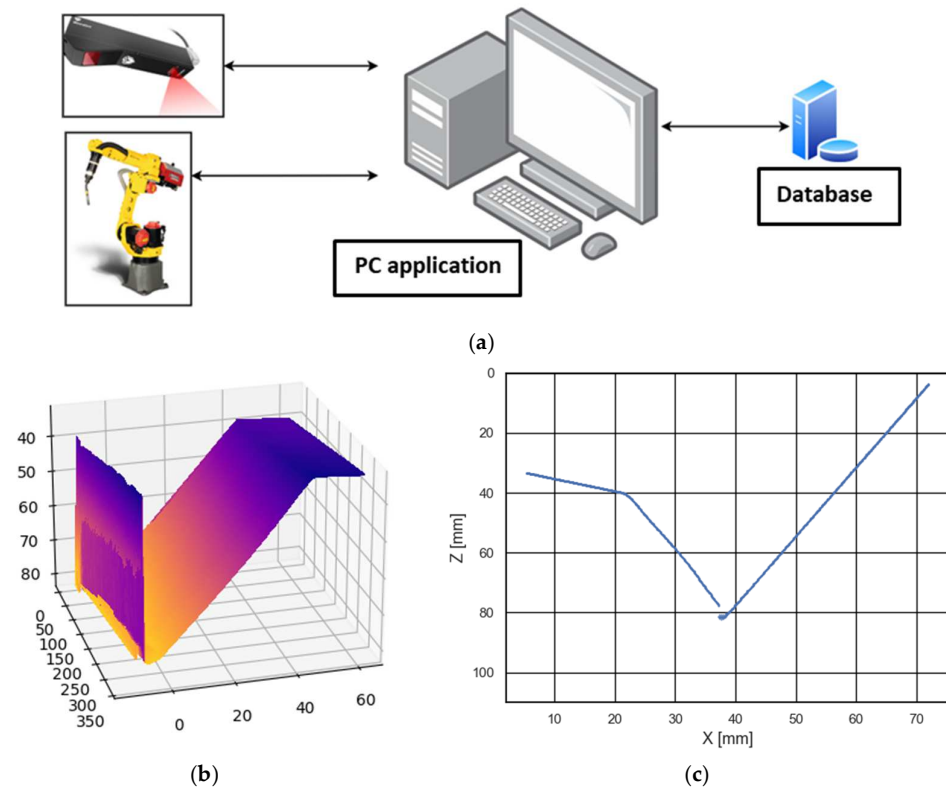


**Figure 2.** (a) Data acquisition chain for the developed intelligent and adaptive welding system; (b) three-dimensional reconstruction of the acquired profiles; (c) discrete profile of the joint.

To initiate the process, a scanning sequence of the weld joint was performed with the robot in the position shown in Figure 1c, scanning the entire length of the joint. Figure 2b shows the 3D reconstruction of the joint based on the 2D profiles acquired by the laser profilometer. For each welding layer, a profile was stored every 20 mm scanned along the joint. From these profiles, the algorithm developed in this work calculated the welding points, i.e., the points that the torch will travel to weld the joint.

Figure 2c shows the point clouds of the equidistant discrete profiles recorded by the laser to cover the length of the joint. Although the profile shown in Figure 2c appears remarkably clear and has minimal noise, it is recognized that this type of laser profilometer inspection has general sources of uncertainty in the process. These sources of uncertainty manifest themselves in several facets. First, there was the possible presence of outliers in the point cloud dataset, which requires meticulous filtering procedures for their elimination. In addition, inherent misalignments in the profiles themselves could indicate cases in which the joint alignment does not exactly match the designated laser trajectory due to hold-ups in the mechanical system of attaching the sensor to the robot. This last point required frequent calibration of the system.

### 3. Results

#### 3.1. Influence of Welding Parameters

The welding process plays a crucial role in achieving strong and reliable joints, especially in applications involving thick plates and delicate ceramic components. In this study, we delved into the influential factors affecting the welding of the first layer of a joint subjected to a 45° bevel angle (Figure 1b). The primary objective of this initial layer was to effectively fill the gap of 3–4 mm between the thick plates housing the ceramic material,



which demands precise control of the welding parameters. To enhance joint filling, we investigated the impact of introducing an oscillation in the welding trajectory. Additionally, we explored the significance of the torch orientation, as an improper inclination could lead to potential collisions with the joint walls. The nominal inclination of the torch stood at  $22.5^\circ$ , but this study involved an analysis of various inclination angles. Detailed information on the range of values examined for the oscillation amplitude and torch inclination can be found in Table 1. By meticulously studying the effects of these critical parameters, we aimed to provide valuable insights for optimizing the welding process in ceramic-plate joints, ultimately ensuring robust and defect-free welds. The subsequent figure, Figure 3, offers visual representations of the scanned profiles for the cases under consideration, providing an initial glimpse into the influence of the welding parameters on the joint filling process.

**Table 1.** Variation of the most critical parameters of the welding process for the analysis of their influence.

Analyzed Parameter	Minimum Value	Maximum Value	Increment
Oscillation amplitude (A)	0 mm	3 mm	1 mm
Angle variation ( $\alpha$ )	$-3^\circ$	$3^\circ$	$1^\circ$

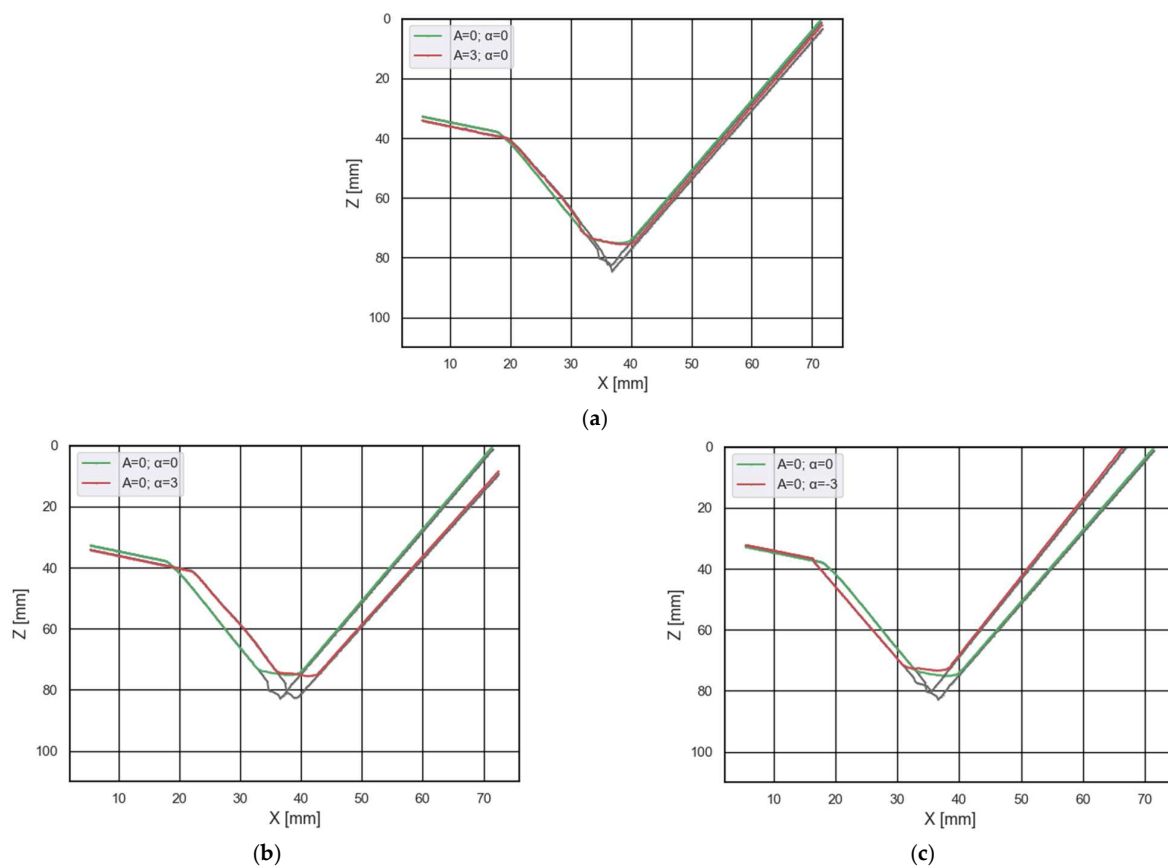


**Figure 3.** (a) Profiles acquired after depositing the first bead with an oscillation amplitude of 0 mm and 3 mm; (b) Profiles acquired after depositing the first bead with a variation of the torch inclination angle of  $0^\circ$  and  $3^\circ$ ; (c) Profiles acquired after depositing the first bead with a variation of the torch inclination angle of  $0^\circ$  and  $-3^\circ$ .

In this work, initially, an experimental study was conducted analyzing the influence of the two most critical parameters in the welding of the first layer of the analyzed joint (Figure 1b). This first layer needed to fill a gap of 3–4 mm between the thick plates where the ceramic was placed. In order to ensure proper material deposition and distribution, a

perpendicular oscillation into the welding trajectory was introduced. This oscillation did not induce any variation in the torch height within the robot's global coordinate framework. Specifically, in this section, the influence of the oscillation amplitude value was studied to observe its effect. On the other hand, another critical parameter was the orientation of the torch, as the bevel angle of the joint was  $45^\circ$ , and the torch could collide with the joint walls. The nominal inclination of the torch was  $22.5^\circ$ , but the influence of varying this inclination was analyzed. The range of values analyzed for the oscillation and angle variation parameters can be observed in Table 1.

In the following figure, the scanned profiles of the proposed cases can be observed. As can be seen in Figure 3a, the change in oscillation amplitude from 0 to 3 mm did not affect the joint filling shape, and the height reached by the first bead was similar. There was also no apparent influence from the variation in the torch inclination angle, as observed in Figure 3b,c. In conclusion, it was confirmed that the influence of oscillation amplitude and variation of the torch inclination angle within the analyzed range was negligible. Therefore, the system validation tests were conducted with an oscillation amplitude of 0 mm and a variation in the torch inclination angle of  $0^\circ$ .

### 3.2. System Learning

The approach described in this section was based on combining the experience of a skilled operator with a machine learning system to develop an intelligent solution for welding thick joints. To achieve this, before developing an algorithm that automatically selected the welding points based on the profiles acquired by the laser, an expert operator was asked to indicate the optimal welding points based on the geometric shape of the profiles. For this purpose, the operator used a solution similar to the one presented in Section 2, implementing a "click and go" approach. In this way, the system had an intuitive user interface that allowed the expert operator to visualize the acquired profiles and select the optimal welding points. During this process, the coordinates of these points were recorded together with the acquired profiles. These data were later used to design the prediction algorithm and validate the obtained results.

### 3.3. Automatic Determination of the Welding Trajectory

In this section, the methodology used for the development of an algorithm that automatically selected the welding points is described, starting from the treatment of the profile acquired by the laser profilometer, continuing with the determination of the welding points, and finally, determining their implications in defining the torch positions for welding the first bead.

#### 3.3.1. Processing of the Acquired Profiles

Once the thick joints were scanned to weld the first bead, point clouds were obtained. As can be observed, the empty joint before welding the first bead had a V shape, and the weld should go through the middle. Since performing a numerical analysis with a point cloud was too challenging, polynomial interpolation and curve fitting were proposed as solutions to work with the profile. In this way, a curve or mathematical function (Equation (1)) was constructed that best fits the available series of data. However, as an approximation, there was always an error calculated using Equation (2).

$$P_n(x) = f(x_0) + f'(x_0)(x - x_0) + \left(\frac{1}{2!}\right)f''(x_0)(x - x_0)^2 + \dots + (1/n!)f^{(n)}(x_0)(x - x_0)^n \quad (1)$$

$$f(x) - P_n(x) = R_n(x) = (1/(n+1)!)f^{(n+1)}(\varepsilon)(x - x_0)^{n+1} \quad (2)$$

where  $n$  is the degree of the polynomial. This polynomial, defined by Equation (1), had the desired degree. To determine the optimal degree, a sensitivity study was conducted, testing polynomials of different degrees. The polynomial of degree 15 was the minimum degree polynomial, which significantly reduced the difference in error. As the degree increased,

the approximation of the regression of the points improved. However, working with a higher degree polynomial became more challenging because the number of roots increased, and the polynomial became too wavy. On the other hand, it was determined that this polynomial must have a minimum degree of 4 because, if it is lower, the function will not have at least two inflection points to work with, or the working areas of the polynomial will be too wide, and the accuracy will not be sufficient. Therefore, it is important to strike a balance, which in this case was achieved with a polynomial degree of 15 (Figure 4).

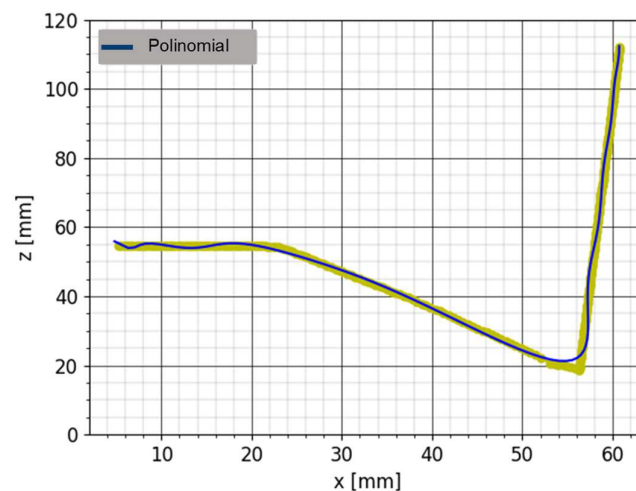


**Figure 4.** Stage of processing the measured profile by the laser profilometer, where the data is approximated to a polynomial of degree 15.

### 3.3.2. Determination of the Welding Points

For the determination of the optimal welding points and to be able to plan the torch path, it was beneficial to acquire the characteristic points of the joint profile. First, the characteristic points of the polynomial defined in the previous section were identified.

The minimum point of the polynomial was useful not only for positioning the torch in each weld but also for defining the inclination of the torch to be applied. To search for this point of the polynomial, the roots of the derivative were calculated. These roots were filtered to choose the relevant ones, as those that were close to the area of the optimal torch position were retained. In this case, the minimum point of the polynomial created in the previous section (Figure 5 in blue) can be seen in Figure 5 in yellow.

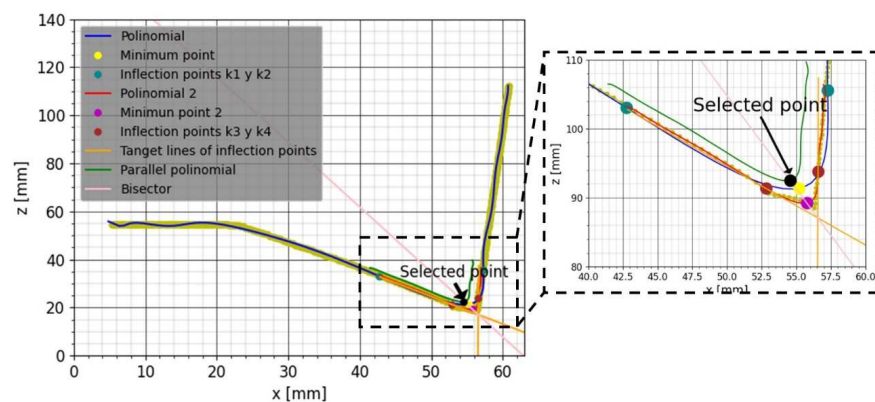


**Figure 5.** Procedure for the selection of welding points.

Regarding the inflection points of the polynomial, it was necessary to calculate the second derivative. Once the list of inflection points was obtained, they were filtered, and only the first inflection point to the left of the minimum point and the first inflection point



to the right of the minimum point were considered. These points can be seen in Figure 5 in cyan.

$$f''(k) \geq 0, f''(k+1) \leq 0 \text{ Inflection point } k : k1 \quad (3)$$

$$f''(k) \leq 0, f''(k+1) \geq 0 \text{ Inflection point } k : k2 \quad (4)$$

Once the inflection points were calculated, the hot area (where the welding point is located) was defined as the area between the two inflection points. Another polynomial fitting was performed with the remaining profile points within this zone to obtain a more accurate approximation (Figure 5, polynomial in red). To continue, the three characteristic points of this new polynomial were recalculated: the minimum point (Figure 5, in pink) and the two inflection points (Figure 5, in maroon).

Since the objective of the welding process is to fill the joint, and both inflection points were prominent for this joint, a “midpoint” between these two points was sought as the selected point. To accomplish this, two tangent lines were calculated from both inflection points ( $k3$  and  $k4$ ), and the bisector of these two tangent lines was drawn, as shown in Figure 5, in pink. Along the bisector lies the optimum point for torch placement, but the distance from this point to the minimum point remains unknown.

From the data stored through the machine learning system (Section 3.2), where an expert operator views some profiles and clicks on the optimal welding point, the average of all distances from the minimum point to the welding point was calculated. Using this average value, a polynomial parallel to the adjustment polynomial was created, shifting the adjustment polynomial by that average value (Figure 5, polynomial in green). The selected point, i.e., the optimum welding point where the torch (specifically the tip of the wire) should be placed for proper welding, would be where this shifted polynomial intersects with the bisector.

In summary, through this methodology, an algorithm was created that, starting from the point cloud of a discrete profile acquired by the laser profilometer, selected the optimal points for torch placement for welding the first layer of the joint.

### 3.3.3. Welding Path Generation

Once the procedure for obtaining welding points from a discrete profile of the joint was defined, the system applied the same algorithm to all the profiles that were acquired along the joint. By connecting these selected points, the optimal welding path was generated, as shown in the following Figure 6.

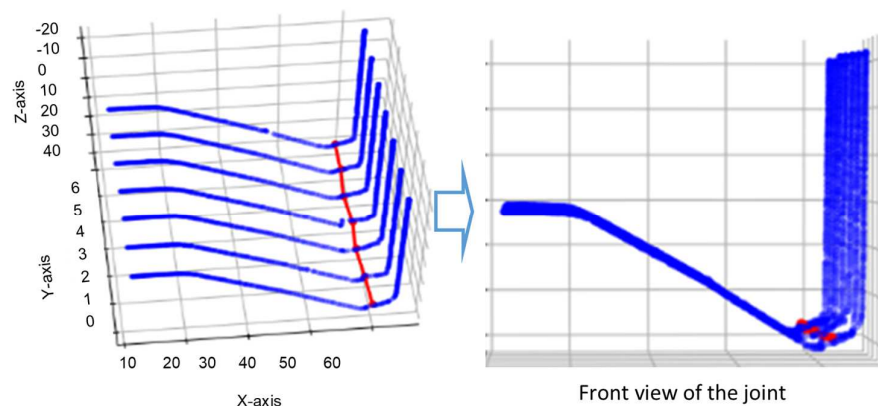


**Figure 6.** Welding path generation.

### 3.4. Validation of the System

Finally, in order to validate the automated and intelligent robotic solution designed for the welding of very thick joints, two procedures were carried out. For the validation, a T-type joint was used as in the definition of the methodology, which can be seen in Figure 7b, with the joint fully welded along its entire length (similar to the trajectories seen in Figure 6

positioned in the symmetrical position). In Figure 7a, a zoom of the joint area is shown (similar to the one seen in Figure 5). First, the development of the automatic spot weld selection algorithm was validated by comparing the welding spots selected by the expert operator and the algorithm developed on the same scanned joint. As shown in Figure 7a, the points chosen by the operator and those forecasted by the system exhibited similarity and validity. It is important to note that in this case of welding, very high precision is not required.

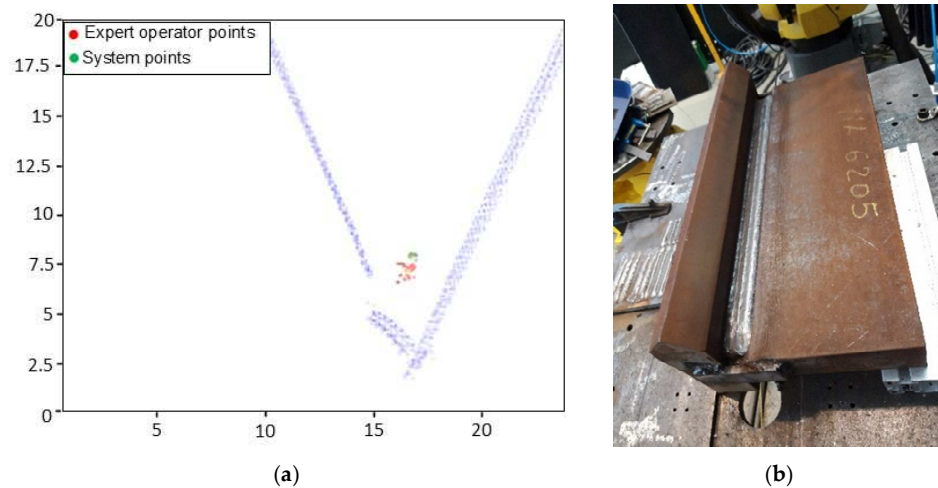


**Figure 7.** Validation of the developed system: (a) Comparison of points selected by an expert operator and by the adaptive and intelligent system developed in this research; (b) Joint welded using the developed system.

Second, as a final validation, a joint with complete T-shaped geometry (Figure 7b) was welded using the developed automatic, intelligent, and adaptive robotic system within this work, generating the trajectories of the first layer with the developed algorithm.

Figure 7a reveals a wider dispersion of system points compared to those meticulously selected by the operator. It is crucial to determine the magnitude of the impact resulting from this wider scatter of spots on the quality of the welded joint. It is also important to consider whether this wider distribution of spots introduces discernible variations in the structural integrity or mechanical characteristics of the final weld. Figure 7b serves as a tangible exemplification of the developed algorithm's merits. Notably, the solution derived from the system points converges toward a height consistency that mirrors the intrinsic nature of the actual joint. Conversely, the solution attained by the skilled operator forms a diffuse cloud with closely clustered points. The crux of the matter emerges in Figure 7b, where the welded joint is showcased. This portrayal vividly demonstrates the algorithm's advantages: the delineated trajectory adheres more closely to the actual joint's geometry, a geometry presupposed as a straight line based on technical specifications. This alignment is accomplished automatically, yielding a consequential reduction in time expenditure.

Finally, a salient feature is the system's potential for operator intervention. This provision accommodates adjustments or the introduction of trajectories by the operator, thereby harmonizing the automated precision of the system with the judicious oversight and expertise of the operator. This thoughtful integration thus synergizes efficiency and expertise, ultimately enriching the welding process.

#### 4. Conclusions

In conclusion, this work developed an automated and adaptable robotic system for welding joints with large thicknesses. The system was based on the use of a laser profilometer and an algorithm for searching for optimal welding positions based on the data acquired by the laser. The following were the main conclusions of this work:

1. This automated and adaptable robotic system was intricately designed and implemented at both the physical and communication levels. In the physical domain, meticulous integration of the sensor, including precise mechanical alignment and thorough calibration, ensured accurate data collection during welding. Meanwhile, the establishment of robust communication protocols facilitated seamless real-time coordination among system components. Complementing this, sophisticated software algorithms drove decision-making and task execution, resulting in a cohesive, high-performance robotic system ready to enhance industrial and technological applications.
2. This system was applied in the field of welding of large thickness joints since the automation and adaptability of the robotic system developed allowed greater efficiency and precision in the welding process. Additionally, by using real-time acquired profiles, the system could adapt to different joint geometries and even deformations arising during welding or due to incorrect assembly, making it versatile and flexible.
3. For welding “T”-shaped joints with large thicknesses, it was confirmed that the amplitude of oscillation and variation in the torch’s tilt angle in the analyzed range had no influence on the welding of the first layer of such joints.
4. For welding this type of joint, the developed system was able to automatically generate the torch trajectory for welding the first layer based on the profiles acquired by laser profilometer. To achieve this, a robust and precise algorithm for selecting optimal welding points was developed.
5. The developed system was validated in two ways, achieving satisfactory results. On the one hand, the automatically selected welding points through the algorithm were compared to the welding points selected by an expert operator, yielding similar results. On the other hand, a real joint was welded, achieving a quality weld.

In summary, this study offers a significant contribution to the development of advanced automated solutions for welding joints with large thicknesses, thereby improving efficiency, precision, and adaptability. Therefore, these alternatives have become a viable option to replace the manual welding used today. As future lines of research, algorithms could be developed for predicting points for additional layers of joints, enabling the automatic welding of the entire joint, and also analyzing other geometries of joints with large thicknesses.

The work presented in this paper lays the foundation for future research and development in the field of welding process automation. While we have demonstrated the effectiveness of our approach in the context of T-shaped joints and specific welding conditions, we acknowledge the potential to extend this methodology to a variety of joint geometries and welding scenarios. In forthcoming endeavors, we plan to explore the adaptability of our method across different setups, including joints of varying sizes and materials, as well as diverse welding conditions. Additionally, we will consider optimizing key parameters and integrating advanced machine learning techniques to achieve enhanced autonomy and precision in the welding process. These investigations hold the promise of delivering innovative and versatile solutions to address a wide range of challenges in the welding and manufacturing industry.

**Author Contributions:** Conceptualization, F.V., A.S. and E.A.; Data curation, F.V., A.S. and E.A.; Formal analysis, F.V., D.C. and E.A.; Investigation, F.V., A.S. and E.A.; Methodology, F.V., D.C. and E.A.; Project administration, A.S.; Supervision, A.S.; Validation, D.C., P.V. and A.S.; Writing—original draft, F.V. and D.C.; Writing—review and editing, F.V., D.C., P.V., A.S. and E.A. All authors have read and agreed to the published version of the manuscript.

**Funding:** The authors acknowledge the Basque Government for financing the H2OCEAN project, HAZITEK 2021 program [ZE-2021/00037] and HYSHORE project HAZITEK 2021 program [ZE-2021/00032].

**Institutional Review Board Statement:** Not applicable.

**Informed Consent Statement:** Not applicable.

**Data Availability Statement:** The data presented in this study are available on request from the corresponding author.

**Conflicts of Interest:** The authors declare no conflict of interest.

## References

1. Pattanayak, S.; Sahoo, S.K. Gas metal arc welding based additive manufacturing—A review. *CIRP J. Manuf. Sci. Technol.* **2021**, *33*, 398–442. [[CrossRef](#)]
2. Palani, P.K.; Murugan, N. Optimization of weld bead geometry for stainless steel claddings deposited by FCAW. *J. Mater. Process. Technol.* **2007**, *190*, 291–299. [[CrossRef](#)]
3. Gonçalves, C.V.; Vilarinho, L.O.; Scotti, A.; Guimarães, G. Estimation of heat source and thermal efficiency in GTAW process by using inverse techniques. *J. Mater. Process. Technol.* **2006**, *172*, 42–51. [[CrossRef](#)]
4. Mahapatra, M.M.; Datta, G.L.; Pradhan, B.; Mandal, N.R. Three-dimensional finite element analysis to predict the effects of SAW process parameters on temperature distribution and angular distortions in single-pass butt joints with top and bottom reinforcements. *Int. J. Press. Vessel. Pip.* **2006**, *83*, 721–729. [[CrossRef](#)]
5. Curiel, D.; Veiga, F.; Suarez, A.; Villanueva, P. Advances in Robotic Welding for Metallic Materials: Application of Inspection, Modeling, Monitoring and Automation Techniques. *Metals* **2023**, *13*, 711. [[CrossRef](#)]
6. Yang, C.; Ye, Z.; Chen, Y.; Zhong, J.; Chen, S. Multi-pass path planning for thick plate by DSAW based on vision sensor. *Sens. Rev.* **2014**, *34*, 416–423. [[CrossRef](#)]
7. Chen, C.; Hu, S.; He, D.; Shen, J. An approach to the path planning of tube-sphere intersection welds with the robot dedicated to J-groove joints. *Robot. Comput. Integr. Manuf.* **2013**, *29*, 41–48. [[CrossRef](#)]
8. Shi, L.; Tian, X. Automation of main pipe-rotating welding scheme for intersecting pipes. *Int. J. Adv. Manuf. Technol.* **2015**, *77*, 955–964. [[CrossRef](#)]
9. Ye, G.; Guo, J.; Sun, Z.; Li, C.; Zhong, S. Weld bead recognition using laser vision with model-based classification. *Robot Comput. Integr. Manuf.* **2018**, *52*, 9–16. [[CrossRef](#)]
10. He, Y.; Chen, Y.; Xu, Y.; Huang, Y.; Chen, S. Autonomous Detection of Weld Seam Profiles via a Model of Saliency-Based Visual Attention for Robotic Arc Welding. *J. Intell. Robot. Syst. Theory Appl.* **2016**, *81*, 395–406. [[CrossRef](#)]
11. Girón-Cruz, J.A.; Pinto-Lopera, J.E.; Alfaro, S.C.A. Weld bead geometry real-time control in gas metal arc welding processes using intelligent systems. *Int. J. Adv. Manuf. Technol.* **2022**, *123*, 3871–3884. [[CrossRef](#)]
12. Zhang, Z.; Yu, H.; Lv, N.; Chen, S. Real-time defect detection in pulsed GTAW of Al alloys through on-line spectroscopy. *J. Mater. Process. Technol.* **2013**, *213*, 1146–1156. [[CrossRef](#)]
13. Lv, N.; Xu, Y.; Zhang, Z.; Wang, J.; Chen, B.; Chen, S. Audio sensing and modeling of arc dynamic characteristic during pulsed Al alloy GTAW process. *Sens. Rev.* **2013**, *33*, 141–156. [[CrossRef](#)]
14. Yan, S.J.; Ong, S.K.; Nee, A.Y.C. Optimal Pass Planning for Robotic Welding of Large-dimension Joints with Deep Grooves. In *Procedia CIRP*; Elsevier: Amsterdam, The Netherlands, 2016; pp. 188–192. [[CrossRef](#)]
15. Barborak, D.; Conrardy, C.; Madigan, B.; Paskell, T. “Through-Arc” Process Monitoring Techniques for Control of Automated Gas Metal Arc Welding. In Proceedings of the IEEE International Conference on Robotics and Automation 1999, Detroit, MI, USA, 10–15 May 1999; pp. 3053–3058.
16. Fridenfalk, M.; Bolmsjö, G. Design and Validation of a Sensor Guided Robot Control System for Welding in Shipbuilding. *Int. J. Join. Mater.* **2002**, *14*, 44–55.
17. Kim, C. Through Arc Sensing for Reciprocating Wire Feed Gas Metal Arc Welding. *Proc. Inst. Mech. Eng. Part B J. Eng. Manuf.* **2015**, *229*, 1557–1565. [[CrossRef](#)]
18. Zhou, X.; Wang, X.; Gu, X. Welding Robot Path Planning Problem Based on Discrete MOEA/D with Hybrid Environment Selection. *Neural Comput. Appl.* **2021**, *33*, 12881–12903. [[CrossRef](#)]
19. Ogbemhe, J.; Mpofo, K.; Tlale, N. Optimal Trajectory Scheme for Robotic Welding along Complex Joints Using a Hybrid Multi-Objective Genetic Algorithm. *IEEE Access* **2019**, *7*, 158753–158769. [[CrossRef](#)]
20. Wang, X.; Zhou, X.; Xia, Z.; Gu, X. A Survey of Welding Robot Intelligent Path Optimization. *J. Manuf. Process.* **2021**, *63*, 14–23. [[CrossRef](#)]
21. Rout, A.; Bbvl, D.; Biswal, B.B. Optimal Trajectory Generation of an Industrial Welding Robot with Kinematic and Dynamic Constraints. *Ind. Robot* **2020**, *47*, 68–75. [[CrossRef](#)]
22. Curiel, D.; Veiga, F.; Suarez, A.; Villanueva, P. Methodology for the Path Definition in Multi-Layer Gas Metal Arc Welding (GMAW). *Symmetry* **2023**, *15*, 268. [[CrossRef](#)]

**Disclaimer/Publisher’s Note:** The statements, opinions and data contained in all publications are solely those of the individual author(s) and contributor(s) and not of MDPI and/or the editor(s). MDPI and/or the editor(s) disclaim responsibility for any injury to people or property resulting from any ideas, methods, instructions or products referred to in the content.